

# A Least-Squares Scheme Utilizing Fast Propagating Shock Waves for Early Kick Estimation in Drilling

Haavard Holta and Ole Morten Aamo

**Abstract**—A scheme for fast kick estimation in managed pressure drilling is presented. The reservoir pressure and production index are estimated by utilizing information in a fast traveling shock wave induced by an unexpected rise in reservoir pressure. A least squares estimation problem is formulated from an early-lumping approach based on a reduced order drift-flux model. The Levenberg-Marquardt scheme is applied to solve the non-linear least-squares problem. The estimation scheme is tested with simulated top-side flow measurements from a two-phase drift flux model.

## I. INTRODUCTION

### A. Kick detection and estimation

The well-bore in oil and gas drilling operations can be several kilometers long and extend deep into the earth. Due to a high hydrostatic pressure or trapped high pressure reservoirs, tight pressure control inside the well is important. To control the pressure in the bore-hole, a fluid called drilling mud is circulated down the hollow drilling string, through nozzles on the drill bit and up the annulus which is the open area surrounding the drill-string. A too low pressure in the annulus might lead to an inflow of reservoir fluids, called a *kick*, and/or collapse of the well. If not handled, a kick might lead to blowouts on the surface endangering both the safety of personnel and the drilling rig. The opposite situation with a high annular pressure might lead to fracturing of the well and inflow of drilling mud into the reservoir, potentially damaging the formation. Even more severe, a loss of drilling fluids leads to a loss hydrostatic pressure which in turn might cause a kick further up the annulus.

In *conventional drilling* the annular pressure is controlled by varying the density of the drilling mud. However, with a circulation speed in the magnitude of  $\sim 1 \text{ m s}^{-1}$ , this process is too slow to handle an unexpected rise in reservoir pressure and the resulting kick. Instead, various time-consuming shut-in and circulation procedures must be initiated. This entails stopping the rotation of the drill-string, lifting the drill-bit up from the well-bottom, closing the top-side annular seal known as a *blow out preventer* (BOP) and circulating out any inflow reservoir fluid.

In *Managed Pressure Drilling* (MPD), a rotating control device seals the annulus top-side at the rig and the drilling fluid exits through a valve. This allows for continuous pressure control while drilling by adjusting the valve opening,

effectively adjusting the top-side pressure. In addition, a *back pressure pump* can be used to maintain the hydrostatic pressure in the case of lost circulation. In addition to being an enabling technology by making wells with tight pressure margins drillable, MPD can be used for fast kick attenuation by actively adjusting topside pressure in response to changes in the down-hole situation. Using MPD, the kick can be attenuated without stopping drilling, avoiding the costly shut-in procedures. However, the topside separator equipment can only handle a limited amount of production fluids. Early kick detection and estimation is therefore essential to prevent the kick from developing in magnitude to a level where shut-in procedures must be initiated. In this paper, the problem of fast reservoir characterization for use in kick attenuation is studied.

### B. Previous work and contribution

Reservoir characterization is an important part of off-line well planning and parameters such as reservoir pressure and permeability can be estimated by an extended Kalman filter [1], a genetic algorithm [2], or, close to the method in the current paper, a least-squares approach [3], [4] where the reservoir permeability and pressure for a set of predefined *zones* are estimated off-line. In [5], [6] a reduced DFM model based on a quasi-equilibrium momentum balance is used for online reservoir characterization. Good estimates of model specific states and parameters are also important to relate the reservoir properties to available top-side measurements. To that end, parameter estimation in a *drift-flux model* (DFM) using a least-squares scheme is presented in [7], and various on-line Kalman filter techniques in [8]–[10]. All of the aforementioned papers are so called early-lumping methods where the distributed model is discretized before estimation methods for finite dimensional systems are applied. In the alternative late-lumping methods, the design is carried out for the original distributed model and the system is only discretized before simulation or computer implementation. For results on using the late-lumping approach called *infinite-dimensional backstepping* for state and parameter estimation, see [11]. In addition to the distributed models, various Kalman filtering methods and moving horizon estimators have been applied on lumped, finite dimensional, models for both bottom-hole pressure estimation and reservoir parameter estimation. See e.g. [12]–[16].

A recurring problem in the aforementioned papers is to achieve parameter convergence. In [4] the bottom-hole pressure is excited by active tests in the form of varying the top-side choke pressure. The model in [5] disregards the high

The authors are with the Department of Engineering Cybernetics, Norwegian University of Science and Technology, Trondheim N-7491, Norway (e-mail: haavard.holta@ntnu.no; aamo@ntnu.no).

Economic support from The Research Council of Norway and Equinor ASA through project no. 255348/E30 Sensors and models for improved kick/loss detection in drilling (Semi-kidd) is gratefully acknowledged.

frequency pressure waves and instead rely on the much slower pressure compression mode and even slower void advection wave (see [17, Section 1.5.1]). This is also true for all lumped order models where both the slow void wave and the fast pressure waves are disregarded. And even though not explicitly stated, as can be seen from the time-scales in the simulation results in e.g. [7] and [9], the information carried in pressure waves are not utilized. In this paper, we aim at utilizing the fast pressure waves propagating with the sound speed of the fluids for early kick estimation. Our hope is that the shock wave caused by a sudden rise in bottom-hole pressure carries enough information (i.e. is sufficiently excited) so that reservoir parameters can be correctly estimated, or at least give the MPD decision system some information to guide an early response attempt for attenuation. We combine an early-lumping approach for a simplified to-phase drift-flux model with a least-squares scheme. Compared to the lumped order models, the distributed nature of the drilling system is preserved. But as opposed to the late-lumping approaches, the finite propagation time property is lost.

### C. Problem formulation

Assume that a gas kick is detected at  $t = t_0$ , that the pressure and flow situation prior to the kick are known with the well initially overbalanced, that is single phased. Assume that the top-side volumetric flow  $y(t)$  is available for all  $t \in [t_0, T]$ ,  $T > t_0$ . Consider the following optimization problem

$$(J^*, p_{res}^*) = \arg \min_{(J, p_{res})} \int_{t_0}^{t_0+T} \|y(\tau) - \hat{y}(\tau)\|^2 d\tau \quad (1a)$$

$$\text{s.t. } \hat{y}(t) = y_{mdl}(t; J, p_{res}) \quad (1b)$$

where  $J$  and  $p_{res}$  are the production index and reservoir pressure which will be defined in the next section and  $y_{mdl}$  is the output from a simplified simulation model. The kick estimation scheme takes the form:

- 1) Normal drilling operation: A single-phase state observer is used to estimate the distributed states.
- 2) Detected kick: Solve the optimization problem (1) repeatedly for increasing  $T \leq t$  utilizing the available measurement  $y(\tau)$  for  $\tau \in [t_0, T]$ .
- 3) Predictions: Use the estimated optimal parameters  $(J^*, p_{res}^*)$  as input to a high fidelity simulator to predict how the gas kick size and location evolves with time, so that for instance time of arrival of gas at the rig, along with the gas amount can be forecast.

## II. MODELING

### A. The drift flux model

We start with the classical drift-flux model (DFM) formulation

$$\partial_t(\alpha_L \rho_L) = -\partial_z(\alpha_L \rho_L v_L) \quad (2a)$$

$$\partial_t(\alpha_G \rho_G) = -\partial_z(\alpha_G \rho_G v_G) \quad (2b)$$

$$\begin{aligned} \partial_t(\alpha_L \rho_L v_L + \alpha_G \rho_G v_G) = & -\partial_z(p + \alpha_L \rho_L v_L^2 + \alpha_G \rho_G v_G^2) \\ & -\rho_M g - f \rho_M v_M \end{aligned} \quad (2c)$$

where mud, oil and water are lumped into a single liquid state with density  $\rho_L$ , volume fraction  $\alpha_L$  and velocity  $v_L$  and the gas phase with density  $\rho_G$  and volume fraction  $\alpha_G$  and velocity  $v_G$  is kept separate. The spatial variable is denoted  $z \in [0, L]$  such that  $z = L$  is the top-side choke position, and the time variable is  $t \geq 0$ . The mean density  $\rho_M$  and mean velocity  $v_M$  are defined as

$$\rho_M := \alpha_G \rho_G + \alpha_L \rho_L \quad v_M := \alpha_G v_G + \alpha_L v_L. \quad (3)$$

In addition, since the liquid and gas phase are lumped into a single momentum balance, a set of closure relations must be specified. The pressure  $p$  is related to the densities by

$$\rho_G = \frac{p}{c_G^2}, \quad \rho_L = \rho_{L,0} + \frac{p - p_{L,0}}{c_L^2} \quad (4)$$

where  $c_G$  and  $c_L$  are the sound velocity in gas and liquid phase respectively and  $p_{L,0}$  and  $\rho_{L,0}$  are given constants. The gas and liquid velocities are related by the slip law

$$v_G = \frac{v_M}{1 - \alpha_L^*} + v_\infty \quad (5)$$

where  $\alpha_L^*$  and  $v_\infty$  are empirically estimated constant parameters. Moreover, the former act as a lower bound on  $\alpha_L$  as it was shown in [18] that the DFM is hyperbolic for  $\alpha_L > \alpha_L^*$ .

We assume reservoir in- or out-flow only at the bottom-hole location  $z = 0$  such that the boundary condition takes the form

$$\alpha_L \rho_L v_L + \alpha_G \rho_G v_G = \frac{1}{A} (W_{L,res} + W_{G,res} + W_{L,bit}) \quad (6)$$

where  $A$  is the cross-sectional area of the annulus,  $W_{L,res}$  and  $W_{G,res}$  are the mass influx rate of formation liquid and formation gas respectively, and  $W_{L,bit}$  is the mud mass rate circulation through the drill-bit. Within normal operating conditions during MPD, the inflows are usually modeled by the simple affine relationships

$$W_{L,res} = J_L \rho_L (p_{res} - p(0, t)) \quad (7a)$$

$$W_{G,res} = J_G \rho_G (p_{res} - p(0, t)) \quad (7b)$$

where  $J_L$  and  $J_G$  are the so-called *production indices* (PI) and  $p_{res}$  is the reservoir pressure. In the following, we assume that both the PI's  $J_G$  and  $J_L$  and the reservoir pressure are unknown. For the top-side boundary condition, we ignore the choke dynamics and assume the MPD system operates under set-point pressure control. That is

$$p(L, t) = p_s \quad (8)$$

for a constant set-point  $p_s$ .

### B. Model reduction and Riemann invariants

Following the approach in [19] and [5], by defining the *pseudo density*

$$\rho = \rho_M - \alpha_L^* \rho_L, \quad (9)$$

the *pseudo mass concentration*

$$\chi = \frac{(\alpha_L - \alpha_L^*) \rho_L}{\rho_M - \alpha_L^* \rho_L}, \quad (10)$$

and neglecting higher order terms, it can be shown that system (2) can be written in terms of the coordinates  $s = (\chi, \rho, v_G)$  as

$$\partial_t \chi + v_G \partial_z \chi = 0 \quad (11a)$$

$$\partial_t \rho + v_G \partial_z \rho + \rho \partial_z v_G = 0 \quad (11b)$$

$$\partial_t v_G + \frac{\bar{\alpha}_0(s) c_M^2(s)}{\rho} \partial_z \chi + \frac{c_M^2(s)}{\rho} \partial_z \rho + v_G \partial_z v_G = S(s) \quad (11c)$$

where

$$\bar{\alpha}_0 := \frac{\rho(\rho_G - \rho_L)}{\rho_L(1 - \alpha_L^*)\rho_G}, \quad c_M^2(s) := \frac{(1 - \alpha_L^*)p}{\alpha_G \rho} \quad (12)$$

and

$$\begin{aligned} S(s) &:= -\frac{\rho_M}{\rho} g - f \frac{\rho_M}{\rho} v_M \\ &= -\left(1 + \frac{\alpha_L^* \rho_L}{\rho}\right) \left(g - \frac{f}{\rho} (1 - \alpha_L^*) (v_G - v_\infty)\right). \end{aligned} \quad (13)$$

Observe that the pseudo mass concentration  $\chi$  is a *Riemann invariant* propagating with speed  $v_G$ . Following [20], the two other eigenvalues, denoted  $\lambda$  and  $-\mu$ , are given by

$$\lambda(s) = v_G + c_M(s), \quad -\mu(s) = v_G - c_M(s). \quad (14)$$

Since  $c_M \gg v_G$ , for high frequencies the pseudo mass concentration  $\chi$  can be considered constant. The pressure wave dynamics (11b) and (11c) with eigenvalues  $\lambda$  and  $\mu$  can then be considered decoupled from the void fraction wave (11a) with eigenvalue  $v_G$ . The system can now be written in terms of the Riemann invariants  $(u, v)^T := V(\rho, v_G)^T$ , where

$$V := \frac{1}{2} \begin{bmatrix} \frac{c_M}{\rho} & 1 \\ -\frac{c_M}{\rho} & 1 \end{bmatrix} \quad (15)$$

is the set of left eigenvectors corresponding to  $\Lambda := \text{diag}(\lambda, -\mu)$ , yielding the reduced order *quasi-linear* system on Riemann form

$$\partial_t \begin{bmatrix} u \\ v \end{bmatrix} + \Lambda(\chi; u, v) \partial_x \begin{bmatrix} u \\ v \end{bmatrix} = \begin{bmatrix} \tilde{S}(\chi; u, v) \\ \tilde{S}(\chi; u, v) \end{bmatrix} \quad (16)$$

where

$$\begin{aligned} \tilde{S}(\chi; u, v) &= \frac{1}{2} S(V^{-1}(u, v)^T) \\ &\quad - \frac{\bar{\alpha}_0(V^{-1}(u, v)^T) c_M^2(V^{-1}(u, v)^T)}{2\rho} \partial_z \chi. \end{aligned} \quad (17)$$

Next, we heuristically simplify the coefficient matrix  $\Lambda(s)$  to be independent of the state  $u$  representing the fast pressure wave. First, since  $c_M \gg v_G$ , we set  $\lambda = \mu = c_m^2$ . Second, the sound velocity model (12) is derived assuming the liquid is incompressible. This assumption can not be used to model transitions between single to two-phase flows as the pressure is undefined for  $\alpha_G = 0$ . To model such transitions, [21] propose to use the switching model

$$\lambda = \mu = \begin{cases} c_L, & \text{if } \alpha_G < \varepsilon \\ c_M, & \text{if } \varepsilon \leq \alpha_G < 1 - \alpha_L^* \end{cases} \quad (18)$$

where  $\varepsilon > 0$  is a small parameter. The case  $\lambda = \mu = c_L$  for  $\alpha_G < \varepsilon$  follows easily when computing the eigenvalues of

(2) in the limiting case  $\alpha_G \rho_G \ll \alpha_L \rho_L$ , which as expected corresponds to the eigenvalues in the corresponding single-phase flow model. Lastly, observing that  $c_M^2$  in (12) can be written on the form

$$c_M^2 = \frac{1 - \alpha_L^*}{\alpha_G^2} c_G^2 (1 - \chi) \quad (19)$$

and that  $\alpha_G(s) \approx \alpha_G(\chi, \bar{\rho}, \bar{v}_G)$  where  $(\bar{\rho}, \bar{v}_G)$  are the steady state values of  $(\rho, v_G)$  for constant  $\chi$ , we have  $\alpha \approx \alpha(\chi)$ , so that  $c_M \approx c_M(\chi)$  and  $\Lambda \approx \Lambda(\chi)$ . That is, the quasi-linear system (16) can be approximated by the *semi-linear* system

$$\partial_t \begin{bmatrix} u \\ v \end{bmatrix} + \Lambda(\chi) \partial_x \begin{bmatrix} u \\ v \end{bmatrix} = \begin{bmatrix} \tilde{S}(\chi; u, v) \\ \tilde{S}(\chi; u, v) \end{bmatrix} \quad (20)$$

for constant  $\chi$ .

Similarly to the eigenvalues, we consider two separate cases for the down-hole boundary conditions: (1) A gas kick, i.e.  $J_L = 0$ ,  $\alpha_G(0, t) = 1$ , and (2) a liquid kick, i.e.  $J_G = 0$ ,  $\alpha_L(0, t) = 1$ . Assuming incompressible liquid, we have for (1)

$$v_G(0, t) = \frac{J_G}{A} (p_{res} - p(0, t)) \quad (21)$$

$$= \frac{J_G c_G \rho}{A} \rho(0, t) + \frac{J_G}{A} (p_{res} - c_G^2 \alpha_L^* \rho_L). \quad (22)$$

Applying the transformation  $(u, v)^T = V(\rho, v_G)^T$  yields

$$u(0, t) = \theta_1 v(0, t) + \theta_2 \quad (23)$$

where

$$\theta_1 = \frac{(J \frac{c_G \rho_G}{A} - 1)}{(J \frac{c_G \rho_G}{A} + 1)}, \quad \theta_2 = \frac{J p_r + q_{bit}}{(J \frac{c_G \rho_G}{A} + 1)}. \quad (24)$$

For (2), we get the same structure (23), but with

$$\theta_1 = \frac{(J \frac{c_L \rho_L}{A} - 1)}{(J \frac{c_L \rho_L}{A} + 1)}, \quad \theta_2 = \frac{J p_r + q_{bit}}{(J \frac{c_L \rho_L}{A} + 1)}. \quad (25)$$

The top-side boundary condition (8) in  $(u_1, u_2)$ -coordinates is given by

$$v(L, t) = u(L, t) + \sigma \quad (26)$$

where  $\sigma = -\frac{c_L}{\rho} p_s$ . The top side measurement  $y_{mdi}(t) = A v_L(t)$  used in (1) is

$$y_{mdi}(t) = u(1, t) + v(1, t) + \frac{W_{l, bit}}{\rho_L}. \quad (27)$$

### III. NUMERICAL ESTIMATION SCHEME

#### A. Early lumping discretization

Consider the system (20). Let  $x_1, \dots, x_N$  be uniformly distributed points on  $[0, 1]$  such that  $x_i - x_{i-1} = \frac{1}{N+1} =: \Delta x$  and let  $u_i(t) := u(x_i, t)$ ,  $v_i(t) := v(x_i, t)$ ,  $\chi_i(t) := \chi(x_i, t)$  for  $i = 1, \dots, N$  such that

$$\frac{du_i}{dt} + \lambda(\chi_i) \frac{du_i}{dx} = \tilde{S}(\chi_i; u_i, v_i) \quad (28a)$$

$$\frac{dv_i}{dt} - \mu(\chi_i) \frac{dv_i}{dx} = \tilde{S}(\chi_i; u_i, v_i). \quad (28b)$$

To limit numerical diffusion, the spatial derivatives are approximated using the *linear upwind differencing* scheme

$$\frac{du_i}{dx} = \frac{3u_i - 4u_{i-1} + u_{i-2}}{2\Delta x} \quad (29a)$$

$$\frac{dv_i}{dx} = \frac{-3v_i + 4v_{i+1} - v_{i+2}}{2\Delta x}, \quad (29b)$$

but with the spatial derivatives at the endpoints, as a special case, computed using the first order upwind scheme

$$\frac{du_1}{dx} = \frac{u_1 - u_0}{\Delta x} \quad (30a)$$

$$\frac{dv_N}{dx} = \frac{v_{N+1} - v_N}{\Delta x} \quad (30b)$$

where the endpoints are found by extrapolation as

$$u_0(t) = \theta_1 v_0(t) + \theta_2 \quad (31)$$

$$\approx \theta_1 (2v_1(t) - v_2(t)) + \theta_2 \quad (32)$$

and

$$v_{N+1}(t) = u_{N+1}(t) + \sigma \quad (33)$$

$$\approx (2u_N(t) - v_{N-1}(t)) + \sigma. \quad (34)$$

In addition, we approximate the measurement  $y_{mdl}$  in terms of  $v_{N+1}$  and  $u_{N+1}$  as

$$y_{mdl}(t) \approx u_{N+1}(t) + v_{N+1}(t) + q_{bit}. \quad (35)$$

Defining  $w = [u_1, \dots, u_N, v_1, \dots, v_N]$  gives the following set of ODEs on state space form:

$$\dot{w} = A(\chi)w + B_1(\chi)\theta_2 + B_2(\chi)\sigma + C(\chi; w) \quad (36)$$

where

$$A(\chi) = M(\chi) \begin{bmatrix} A_1 & \theta_1 D_1 \\ D_2 & A_2 \end{bmatrix}, \quad (37)$$

$$M(\chi) = \text{diag}(-\lambda(\chi_1), \dots, -\lambda(\chi_N), \mu(\chi_1), \dots, \mu(\chi_N)), \quad (38)$$

$$A_1 = \frac{1}{2\Delta x} \begin{bmatrix} 2 & 0 & 0 & \dots & 0 & 0 & 0 \\ -4 & 3 & 0 & \dots & 0 & 0 & 0 \\ 1 & -4 & 3 & \dots & 0 & 0 & 0 \\ \vdots & \vdots & \vdots & \ddots & \vdots & \vdots & \vdots \\ 0 & 0 & 0 & \dots & 1 & -4 & 3 \end{bmatrix}, \quad (39)$$

$$A_2 = \frac{1}{2\Delta x} \begin{bmatrix} -3 & 4 & -1 & \dots & 0 & 0 & 0 \\ \vdots & \vdots & \vdots & \ddots & \vdots & \vdots & \vdots \\ 0 & 0 & 0 & \dots & -3 & 4 & -1 \\ 0 & 0 & 0 & \dots & 0 & -3 & 4 \\ 0 & 0 & 0 & \dots & 0 & 0 & -2 \end{bmatrix}, \quad (40)$$

$$D_1 = \frac{1}{2\Delta x} \begin{bmatrix} -4 & 2 & 0 & \dots & 0 \\ 2 & -1 & 0 & \dots & 0 \\ \vdots & \vdots & \vdots & \ddots & \vdots \\ 0 & 0 & 0 & \dots & 0 \end{bmatrix}, \quad (41)$$

$$D_2 = \frac{1}{2\Delta x} \begin{bmatrix} 0 & \dots & 0 & 0 & 0 \\ \vdots & \ddots & \vdots & \vdots & \vdots \\ 0 & \dots & 0 & 1 & -2 \\ 0 & \dots & 0 & -2 & 4 \end{bmatrix}, \quad (42)$$

$$B_1(\chi) = \frac{1}{2\Delta x} M(\chi) [-2 \quad 1 \quad 0 \quad \dots \quad 0]^T, \quad (43)$$

$$B_2(\chi) = \frac{1}{2\Delta x} M(\chi) [0 \quad \dots \quad -1 \quad 2]^T, \quad (44)$$

and

$$C(\chi; w) = [\tilde{S}(\chi; w_1) \quad \dots \quad \tilde{S}(\chi; w_N)]^T. \quad (45)$$

*B. The Levenberg-Marquardt scheme and sensitivity computation*

The ODE system (36) can be simulated using any time-explicit solver provided the discretization step  $t_{k+1} - t_k = \Delta t$  satisfies the *Courant-Friedrichs-Lewy condition*

$$\lambda(\chi_i) \frac{\Delta t}{\Delta x} \leq 1, \quad i = 1, \dots, N. \quad (46)$$

The optimization problem (1) can then be formulated as least squares problem by approximating the integral as the sum of the square error  $(y_k - y_{mdl,k})^2$  for all  $k \in [K_0, K]$  such that  $t_K < T - t_0$ , yielding

$$(J^*, p_{res}^*) = \arg \min_{(J, p_{res})} \sum_{k=0}^K (y(t_k) - y_{mdl}(t_k; J, p_{res}))^2. \quad (47a)$$

Let  $\mathcal{F}$  be a vector with the residual elements  $(y(t_k) - y_{mdl}(t_k; J, p_{res}))$  for  $k = 0, \dots, K$  and  $\mathcal{J}$  the Jacobian of  $\mathcal{F}$  with respect to  $(J, p_{res})$ . Let  $\theta = [\theta_1, \theta_2]^T$  so that the solution to (36) can be written as  $w(t) =: f(t; \theta)$ . We have

$$\begin{aligned} \dot{f}_{\theta_1} &= \frac{\partial}{\partial \theta_1} (A(\chi)w + B_1(\chi)\theta_2(t) + B_2(\chi)\sigma(t) + C(\chi; w)) \\ &= A(\chi)f_{\theta_1} + M(\chi) \begin{bmatrix} 0 & D_1 \\ 0 & 0 \end{bmatrix} w + \frac{\partial C(\chi; w)}{\partial w} f_{\theta_1} \end{aligned} \quad (48)$$

and

$$\begin{aligned} \dot{f}_{\theta_2} &= \frac{\partial}{\partial \theta_2} (Aw + B_1\theta_2(t) + B_2\sigma(t) + C(w)) \\ &= Af_{\theta_2} + B_1 + \frac{\partial C(\chi; w)}{\partial w} f_{\theta_2} \end{aligned} \quad (49)$$

with initial conditions

$$f_{\theta_1}(t)|_{t=t_0} = f_{\theta_2}(t)|_{t=t_0} = 0 \quad (50)$$

We are interested in the sensitivity of  $y_{mdl}$  relative to changes in the uncertain parameters  $(J, p_{res})$ . Using (35), we have

$$\frac{\partial y_{mdl}}{\partial (p_{res}, J)} = \frac{\partial y_{mdl}}{\partial w} \frac{\partial w}{\partial \theta} \frac{\partial \theta}{\partial (p_{res}, J)} \quad (51)$$

where the second term is available by integrating (48) to (50). The first and third term follow trivially from (35) and (24) (or (25)) respectively and are given by

$$\frac{\partial y_{mdl}}{\partial w} = [0 \quad \dots \quad 0 \quad 1 \quad 0 \dots \quad 0 \quad \sigma^{-1/2}] \quad (52)$$

and

$$\frac{\partial \theta}{\partial (p_r, J)} = (J \frac{c_i \rho_i}{A} + 1)^{-2} \begin{bmatrix} 0 & 2 \frac{c_i \rho_i}{A} \\ J(J \frac{c_i \rho_i}{A} + 1) & p_r \end{bmatrix} \quad (53)$$

for  $i = \{L, G\}$ . Having computed the Jacobian  $\mathcal{J}$  as

$$\mathcal{J} = \left[ \frac{\partial y_{mdl,k}}{\partial (p_r, J)} \right]_{k=0, \dots, K}, \quad (54)$$

we can compute the search direction  $d$  for the associated linear trust-region subproblem  $\min_d \|\mathcal{J}d + \mathcal{F}\|^2$  subject to  $\|d\| \leq R$  where  $R > 0$  is the trust region radius, as the solution to

$$(\mathcal{J}^T \mathcal{J} + \gamma I)d = -\mathcal{J}^T \mathcal{F} \quad (55a)$$

$$\gamma(R - \|d\|) = 0. \quad (55b)$$

See e.g. [22] for details on the implementation of the Levenberg-Marquardt scheme.

#### IV. SIMULATION

State measurements were generated using the DFM implementation in [23] employing an advection upstream splitting method for the spatial discretization and explicit Euler for time integration. ODE system (36) and sensitivities (48) and (49) used in the estimation scheme were implemented in MATLAB using the method of lines with the `ode45` solver and used as input to the the least-squares solver `lsqcurvefit` for the minimization problem (47).

At time  $t_0 = 10$ s a kick, caused by a step from  $p_{res} = 400$ bar to  $p_{res} = 450$ bar, is simulated. The system is initially in steady state with  $\alpha_L = 1$  for  $t < 10$ s with the following parameters:

$$l = 2500\text{m}, \quad g = 9.81\text{ms}^{-1} \quad (56a)$$

$$c_G = 346.5\text{ms}^{-1}, \quad c_L = 1200\text{ms}^{-1} \quad (56b)$$

$$\rho_{L,0} - p_{L,0}/c_L^2 = 1318\text{kgm}^{-3}, \quad A = 10.8\text{dm}^2 \quad (56c)$$

$$q_{bit} = 18.7\text{dm}^3\text{s}^{-1}, \quad F = 133.2 \quad (56d)$$

$$C_0 = 1.2, \quad v_\infty = 0.75\text{ms}^{-1}. \quad (56e)$$

We use  $N = 20$  discretization steps and a  $\Delta t = 0.01$ s step length in the ODE solver. The re-computation computation interval was set to 1s which is slower than the propagation time through the liquid phase  $L/c_L = 2500/1200\text{s} \approx 2\text{ms}^{-1}$ .

Two cases are simulated. The first for a liquid inflow with  $J_L = 60$  barrels per day per psi and  $J_G = 0$  and the second for a gas inflow with  $J_L = 0$  and  $J_G = 60$  barrels per day per psi. The velocity profile for the two cases are shown in Figure 3 and Figure 4 respectively. For the gas inflow simulation, the gas fraction profile is shown in Figure 2.

In both cases, we use constant  $\chi_i = 0$  for all  $i = 1, \dots, N$ . The validity of this approximation is studied in Figure 1, where the top side flow measurements are compared for the gas inflow simulation, the liquid inflow simulation and the reduced order semi-linear system (20) for the case of having perfect reservoir parameter estimates. As can be seen, the reduced order semi-linear model with  $\chi = 0$  approximates the DFM generated simulation measurements fairly well during the first two waves. However, as the gas fraction is building up in the gas inflow case, the top-side flow is drifting. This is not modeled by the reduced order system when  $\chi$  is kept constant.

Figure 5 and Figure 6 show the estimated parameters for each re-computation. For the liquid inflow case, both the reservoir pressure and PI estimates are close to the true parameter values. For the gas inflow case, acceptable

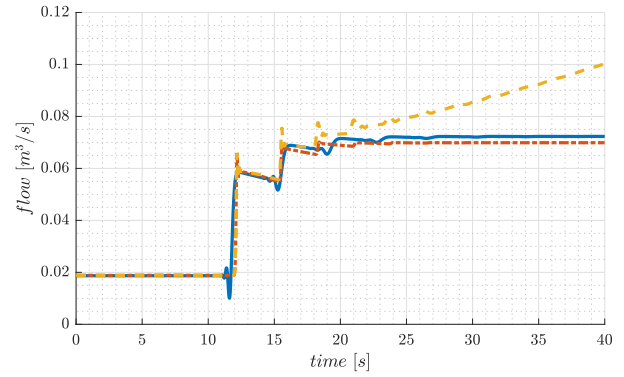


Fig. 1. Reduced order system (20) (solid blue) vs. the full DFM (2) with liquid influx (dash-dotted red) and with gas influx (dashed yellow).

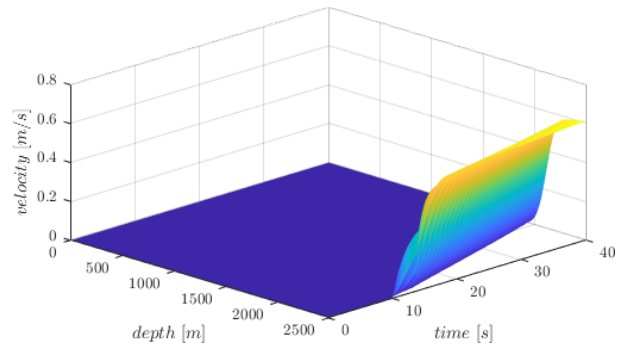


Fig. 2. Gas fraction profile for simulated gas inflow.

reservoir pressure estimates are obtained for most of the re-computations. The production index estimates, however, drift and become unreliable for high gas fractions  $\alpha_G$ .

#### V. CONCLUDING REMARKS

The simulations show that the fast pressure wave dynamics can be used for reservoir characterizations when a kick induced shock wave provide sufficient excitation. However, the scheme should be tested with measurements either from high-fidelity models or real-world data before any strong conclusions on the applicability of the design are made. In a real world implementation, measurement noise and computational cost must be considered. Future work includes implementation of the void fraction wave which can be

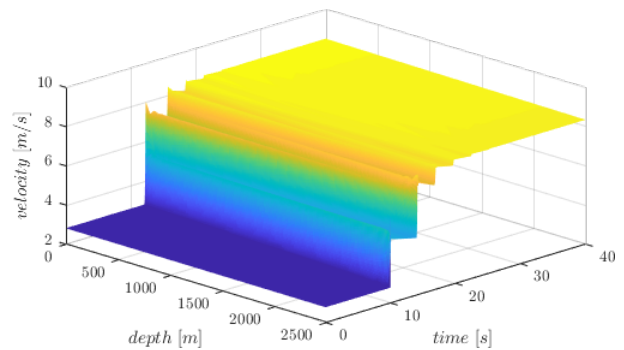


Fig. 3. Velocity profile for simulated liquid influx.

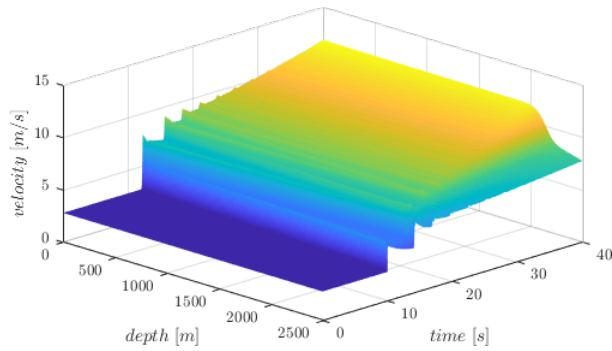


Fig. 4. Velocity profile for simulated gas influx.

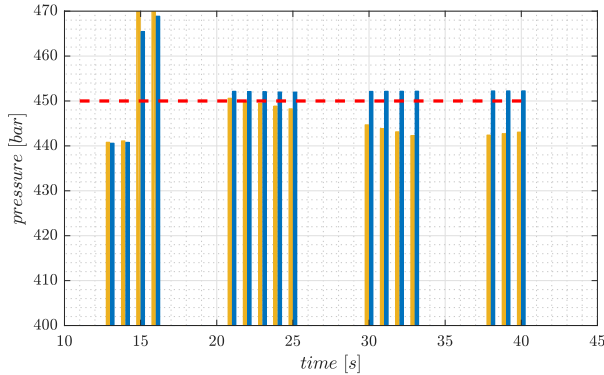


Fig. 5. Estimated reservoir pressure for liquid inflow (blue bars), gas inflow (yellow bars) and true reservoir pressure (red dashed line).

used to provide feed-forward estimates of the pseudo mass concentration  $\chi$ , enabling simulation of the reduced order semi-linear system with a slowly varying gas fraction. The method should also be tested in closed loop with an MPD attenuation controller.

## REFERENCES

- [1] E. H. Vefring, G. Nygaard, R. J. Lorentzen, G. Nævdal, and K. K. Fjelde, "Reservoir characterization during UBD: Methodology and active tests," in *IADC/SPE Underbalanced Technology Conference and Exhibition*. Society of Petroleum Engineers, 2003.
- [2] D. Biswas, P. Suryanarayana, P. Frink, and S. Rahman, "An improved model to predict reservoir characteristics during underbalanced drilling,"

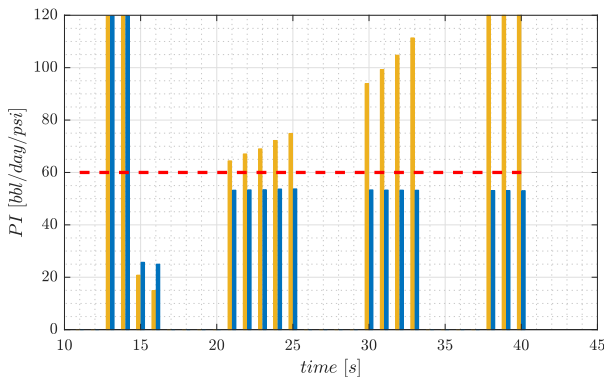


Fig. 6. Estimated production index for liquid inflow (blue bars), gas inflow (yellow bars) and true production index (red dashed line).

- in *SPE Annual Technical Conference and Exhibition*. Society of Petroleum Engineers, 2003.
- [3] E. H. Vefring, G. Nygaard, K. K. Fjelde, R. J. Lorentzen, G. Nævdal, and A. Merlo, "Reservoir characterization during underbalanced drilling: Methodology, accuracy, and necessary data," in *SPE Annual Technical Conference and Exhibition*. Society of Petroleum Engineers, 2002.
- [4] E. H. Vefring, G. H. Nygaard, R. J. Lorentzen, G. Nævdal, and K. K. Fjelde, "Reservoir characterization during underbalanced drilling (UBD): Methodology and active tests," *SPE Journal*, vol. 11, no. 02, pp. 181–192, jun 2006.
- [5] U. J. F. Aarsnes, A. Ambrus, F. D. Meglio, A. K. Vajargah, O. M. Aamo, and E. van Oort, "A simplified two-phase flow model using a quasi-equilibrium momentum balance," *International Journal of Multiphase Flow*, vol. 83, pp. 77–85, jul 2016.
- [6] A. Ambrus, U. J. F. Aarsnes, A. K. Vajargah, B. Akbari, E. van Oort, and O. M. Aamo, "Real-time estimation of reservoir influx rate and pore pressure using a simplified transient two-phase flow model," *Journal of Natural Gas Science and Engineering*, vol. 32, pp. 439–452, 2016.
- [7] R. J. Lorentzen, K. K. Fjelde, J. Frøyen, A. C. Lage, G. Nævdal, and E. H. Vefring, "Underbalanced and low-head drilling operations: Real time interpretation of measured data and operational support," in *SPE Annual Technical Conference and Exhibition*. Society of Petroleum Engineers, 2001.
- [8] R. Lorentzen, G. Nævdal, and A. Lage, "Tuning of parameters in a two-phase flow model using an ensemble kalman filter," *International Journal of Multiphase Flow*, vol. 29, no. 8, pp. 1283–1309, aug 2003.
- [9] A. Nikoofard, U. J. F. Aarsnes, T. A. Johansen, and G.-O. Kaasa, "Estimation of states and parameters of a drift-flux model with unscented kalman filter," *IFAC-PapersOnLine*, vol. 48, no. 6, pp. 165–170, 2015.
- [10] U. J. F. Aarsnes, F. D. Meglio, O. M. Aamo, and G.-O. Kaasa, "Fit-for-purpose modeling for automation of underbalanced drilling operations," in *SPE/IADC Managed Pressure Drilling & Underbalanced Operations Conference & Exhibition*. Society of Petroleum Engineers, 2014.
- [11] H. Anfinsen and O. M. Aamo, *Adaptive Control of Hyperbolic PDEs (Communications and Control Engineering)*. Springer, 2019.
- [12] A. Nikoofard, T. A. Johansen, and G.-O. Kaasa, "Nonlinear moving horizon observer for estimation of states and parameters in underbalanced drilling operations," in *ASME 2014 Dynamic Systems and Control Conference*. ASME, oct 2014.
- [13] —, "Reservoir characterization in under-balanced drilling using low-order lumped model," *Journal of Process Control*, vol. 62, pp. 24–36, feb 2018.
- [14] G. Nygaard, G. Naedal, and S. Mylvaganam, "Evaluating nonlinear kalman filters for parameter estimation in reservoirs during petroleum well drilling," in *2006 IEEE Conference on Computer Aided Control System Design*. IEEE, oct 2006.
- [15] M. Paasche, T. A. Johansen, and L. Imsland, "Regularized and adaptive nonlinear moving horizon estimation of bottomhole pressure during oil well drilling," *IFAC Proceedings Volumes*, vol. 44, no. 1, pp. 10511–10516, jan 2011.
- [16] D. Sui, R. Nybø, G. Gola, D. Roverso, and M. Hoffmann, "Ensemble methods for process monitoring in oil and gas industry operations," *Journal of Natural Gas Science and Engineering*, vol. 3, no. 6, pp. 748–753, dec 2011.
- [17] U. J. F. Aarsnes, "Modeling of two-phase flow for estimation and control of drilling operations," Ph.D. dissertation, NTNU, 2016.
- [18] S. Benzoni-Gavage, "Analyse numérique des modèles hydrodynamiques d'écoulements diphasiques instationnaires dans les réseaux de production pétrolière," Ph.D. dissertation, Lyon 1, 1991.
- [19] S. Gavriluyk and J. Fabre, "Lagrangian coordinates for a drift-flux model of a gas-liquid mixture," *International Journal of Multiphase Flow*, vol. 22, no. 3, pp. 453–460, jun 1996.
- [20] F. Di Meglio, "Dynamics and control of slugging in oil production," Theses, École Nationale Supérieure des Mines de Paris, July 2011.
- [21] K. K. Fjelde, R. Rommetveit, A. Merlo, and A. C. V. M. Lage, "Improvements in dynamic modeling of underbalanced drilling," in *Proceedings of the IADC/SPE Underbalanced Technology Conference and Exhibition*. Houston, Texas: Society of Petroleum Engineers, 2003, p. 8.
- [22] J. J. Moré, "The levenberg-marquardt algorithm: implementation and theory," in *Numerical analysis*. Springer, 1978, pp. 105–116.
- [23] S. Evje and K. K. Fjelde, "Hybrid flux-splitting schemes for a two-phase flow model," *Journal of Computational Physics*, vol. 175, no. 2, pp. 674–701, jan 2002.